JOURNAL OF SOLID STATE CHEMISTRY **133,** 391–399 (1997)
ARTICLE NO. SC977482

A Mixed Valent Molybdenum Monophosphate with a Bidimensional Connection of MoO_6 Octahedra: $Li_3Mo_3O_5(PO_4)_3$

S. Ledain, A. Leclaire, M. M. Borel, J. Provost, and B. Raveau

Laboratoire CRISMAT, UMR 6508, associée au CNRS, ISMRA, et Université de Caen, 6, Boulevard du Maréchal Juin, 14050 Caen Cedex, France

Received December 17, 1996; in revised form May 19, 1997; accepted May 22, 1997

A new mixed-valent molybdenum monophosphate $Li_3Mo_3O_5(PO_4)_3$ with an original structure has been isolated. It crystallizes in the space group $P\bar{1}$ with $a = 11.964$, $b = 12.716$, $c = 8.274$ Å, $\alpha = 90.26°$, $\beta = 96.87°$, and $\gamma = 89.67°$. It is to date the only mixed-valent molybdenum phosphate that exhibits layers of corner-sharing octahedra. The latter, with formulation $[Mo_8O_{37}]_\infty$, are built up of HTB (hexagonal tungsten bronze) rows of octahedra running along b. The 3D $[Mo_3P_3O_{17}]_\infty$ framework results from the stacking of $[Mo_8O_{37}]_\infty$ layers with $[MoPO_7]_\infty$ layers along a, with two successive layers being connected through single PO_4 tetrahedra. Within this framework, the lithium cations exhibit two kinds of coordination, tetrahedral and pyramidal. Examination of the Mo–O distances and the bond valence calculations suggests an ordering of the Mo(V) and Mo(VI) species, but the magnetic susceptibility measurements show a partial electronic delocalization for $T > 10$ K, whereas an antiferromagnetic ordering is evidenced below 7 K. © 1997 Academic Press

INTRODUCTION

The investigation of molybdenum phosphates performed within the last 15 years led to synthesis of nine series of mixed-valent molybdenum phosphates involving the coexistence of Mo(V) and Mo(VI) species in the same matrix. In most of them, molybdenum exhibits bioctahedral units Mo_2O_{11} interconnected through PO_4 tetrahedra as for example in $Li_xMo_2O_3(PO_4)_2$ (1), $LiMo_2O_3(PO_4)_2$ (2), $Cs_3Mo_4P_4O_{22}$ (3), $M_3Mo_4P_4O_{22}$ (M = Rb, Tl) (4), and in several cases isolated units involving MoO_4 tetrahedra or MoO_5 bipyramids as for the $Cs_{8+x}(MoO_4)Mo_{12}O_{18}(PO_4)_{10}\cdot H_2O$ (5), $CsMo_2P_2O_{11}$ (6), $AMo_3P_3O_{16}$ (A = Na, Ag, Li) (7–9), and $AMo_3P_2O_{14}$ (A = K, Na, Ag) (10, 11). It results, for all these compounds, in an ordering of the Mo(V) species that exhibit a specific octahedral configuration and of the Mo(VI) species that adopt either a distorted octahedral, bipyramidal, or tetrahedral coordination. In any case, all these mixed-valent Mo(V)–Mo(VI) phosphates are characterized by an electronic localization due to the fact that the "Mo_n" units are isolated from each other by interconnecting PO_4 tetrahedra. The possibility of an electronic delocalization over molybdenum polyhedra in a mixed-valent molybdenum phosphates is an important issue that requires the synthesis of mixed-valent molybdenum phosphates in which the MoO_6 octahedra would be connected bidimensionally or tridimensionally. Unfortunately, such compounds are to date very rare. The only example deals with the monophosphate $CsMo_6O_{10}(Mo_2O_7)(PO_4)_4$ (12), but in this compound, molybdenum exhibits two coordinations, tetrahedral and octahedral, so that an ordered distribution of Mo(VI) in the dimolybdate groups and in the octahedra and of Mo(V) in the $[Mo_4O_{17}]$ units is again observed.

In order to isolate such compounds, we have explored the Li–Mo–P–O system that was started recently (1, 2, 9, 13, 14) trying to introduce higher Mo(V):Mo(VI) molar ratios. In the present paper we report on a new mixed-valent molybdenum phosphate $Li_3Mo_3O_5(PO_4)_3$, that exhibits an original structure characterized by a 3D octahedral framework for molybdenum. The magnetic properties of this phase are also studied allowing the distribution of the Mo(V) and Mo(VI) species to be discussed.

EXPERIMENTAL SECTION

Chemical Synthesis and Crystal Growth

In order to have a chance to obtain a new phase with a rather high molybdenum (V) content, we have fixed the oxygen content of the nominal compositions for crystal growth in such a way that the Mo(VI):Mo(V) ratio could be varied between 1/2 and 0. In this study, the Li:Mo ratio was systematically fixed to 1, whatever the mixture, and the Mo (or Li):P ratio was systematically varied from 1 to 4. For each mixture a "two-steps method" was used, the temperature of the second step of crystal growth being crucial was varied between 700 and 900 K with various cooling. The resulting products were examined by optical microscopy in order to check the crystallization. Only the crystals

0022-4596/97 $25.00

of good optical quality were selected for the microprobe analysis, and they were tested by X-ray diffraction.

The best results were obtained for a mixture of nominal composition $Li_4Mo_4P_2O_{18}$. The two-steps growth was performed for this composition in the following way: the adequate mixture of MoO_3, $H(NH_4)_2PO_4$, and Li_2CO_3 corresponding to the composition "$Li_4Mo_{3.66}P_2O_{18}$" was first heated in air at 673 K for 2 h in a platinum crucible in order to eliminate CO_2, NH_3, and H_2O. In a second step the appropriate amount of molybdenum (0.33) was added and the finely ground mixture was sealed in an evacuated silica ampoule. The latter was heated for 24 h at 873 K, cooled at 4.3 K hr^{-1} down to 773 K, and finally quenched to room temperature. Black crystals, whose microprobe analysis indicated the molar ratio Mo : P = 1, were extracted from this batch. The lithium content was performed by atomic absorption spectroscopy leading to the molar ratios Mo : P : Li = 1 : 1 : 1, allowing the complete cationic composition to be determined.

The synthesis of the pure phase could only be performed after the structure determination; this allowed the oxygen content to be determined which lead to the composition $Li_3Mo_3P_3O_{17}$. The two steps method was applied: (i) preheating in air of the mixture of nominal composition "$Li_3Mo_{2.66}P_3O_{17}$" (MoO_3, $H(NH_4)_2PO_4$ and Li_2CO_3) in air at 673 K for 2 h, (ii) addition of 0.333 Mo to the first product and heating in evacuated ampoule at 873 K for 24 h.

Elementary Analysis

The analysis of Mo and P was performed with a Tracor microprobe mounted on a JEOL 840 scanning electron microscope.

For the lithium analysis, the crystals were dissolved by boiling in an aqueous mixture of nitric and hydrofluoric acid, and the corresponding solution was investigated by atomic adsorption spectroscopy using a Varian Spectra AA20 spectrometer.

X-Ray Diffraction Study

The powder X-ray diffraction pattern of the monophasic sample was recorded with a Philips diffractometer using Cu$K\alpha$ radiation.

The selection of the crystals was carried out by testing the different crystals that were optically good by the Weissenberg method.

A black crystal with dimensions $0.257 \times 0.032 \times 0.025$ mm^3 was selected for the structure determination. The very small size of the crystal allowed only 4881 reflections with $I > 3\sigma$ among the 14210 measured, so only the nonoxygen and nonlithium atoms may be refined anisotropically.

TABLE 1
Summary of Crystal Data, Intensity Measurements, and Structure Refinement Parameters for $Li_3Mo_3O_5(PO_4)_3$

Crystal data		
Space group	$P\bar{1}$	
Cell dimensions	$a = 11.946(2)$Å	$\alpha = 90.26(1)^\circ$
	$b = 12.716(2)$ Å	$\beta = 96.87(1)^\circ$
	$c = 8.274(1)$ Å	$\gamma = 89.67(1)^\circ$
Volume (Å)	1247.7(3) Å	
Z	4	
ρ_{calc} (gcm^3)	3.585	
Intensity measurements		
λ(Mo$K\alpha$)	0.71073	
Scan mode	ω–θ	
Scan width (°)	$1.2 + 0.35 \tan\theta$	
Slit aperture (mm)	$1.1 + \tan\theta$	
Max θ(°)	45	
Standard reflections	3 measured every 3600 s	
Measured reflections	14210	
Reflections with $I > 3\sigma$	4881	
μ(mm^{-1})	3.46	
Structure solution and refinement		
Parameters refined	300	
Agreement factors	$R = 0.036$	$R_w = 0.044$
Weighting scheme	$w = 1/\sigma^2$	
Δ/σ max	< 0.005	

The cell parameters were determined by diffractometric techniques at 294 K with a least-squares refinement based upon 25 reflections in the range $18^\circ < \theta < 22^\circ$. The data were collected with a CAD4 Enraf Nonius diffractometer with the parameters reported on Table 1. The reflections were corrected for Lorentz and polarization effects and for absorption. The structure was solved with the heavy atom method.

Magnetic Measurements

Magnetic susceptibility measurements were performed on powder samples versus temperature in the range 4.5 to 300 K with a SQUID magnetometer Quantum Design, for an applied magnetic field of 10000 G. The sample was first zero-field cooled, and the magnetic field was applied after the temperature stabilization at 4.5 K.

RESULTS AND DISCUSSION

The refinement of the atomic parameters of the atoms and of the anisotropic thermal factors of Mo and P and the isotropic thermal factors of the other atoms were successful in the space group $P\bar{1}$, leading to the formulation $Li_3Mo_3P_3O_{17}$ with $R = 0.036$ and $R_w = 0.044$ and to the atomic parameters listed in Table 2. Note that the Li atoms were easily located and that their thermal factors are correct. The

TABLE 2
Positional Parameters and Their Estimated Standard Deviations in $Li_3Mo_3O_5(PO_4)_3$

Atom	x	y	z	B(Å^2)
Mo(1)	0.01512(6)	0.11443(6)	0.2432(1)	0.50(2)[a]
Mo(2)	− 0.01346(6)	0.61433(6)	0.2598(1)	0.51(2)[a]
Mo(3)	0.47862(7)	0.61937(6)	0.1838(1)	0.51(2)[a]
Mo(4)	0.60568(6)	0.87233(5)	0.1510(1)	0.44(2)[a]
Mo(5)	0.39953(6)	0.37028(5)	0.34479(9)	0.42(2)[a]
Mo(6)	0.52314(7)	0.11880(6)	0.3206(1)	0.53(2)[a]
P(1)	0.7322(2)	0.4038(2)	0.5956(3)	0.46(4)[a]
P(2)	− 0.0546(2)	0.3621(2)	0.1420(3)	0.34(4)[a]
P(3)	0.0546(2)	0.8614(2)	0.3582(3)	0.42(4)[a]
P(4)	0.2716(2)	0.1558(2)	0.4417(3)	0.46(4)[a]
P(5)	0.2725(2)	0.3515(2)	− 0.0582(3)	0.46(4)[a]
P(6)	0.7357(2)	0.0940(2)	0.1005(3)	0.50(4)[a]
O(1)	0.0742(6)	0.0924(6)	0.074(1)	1.36(8)
O(2)	− 0.0649(6)	0.1536(5)	0.4557(9)	0.88(8)
O(3)	− 0.1432(6)	0.1346(5)	0.1374(9)	0.80(8)
O(4)	0.1586(6)	0.1050(5)	0.3959(9)	0.88(8)
O(5)	0.0250(5)	0.2747(5)	0.2306(8)	0.72(8)
O(6)	− 0.0144(5)	− 0.0365(5)	0.3029(8)	0.64(8)
O(7)	− 0.0737(6)	0.5935(5)	0.4302(9)	1.12(8)
O(8)	0.0660(6)	0.6535(5)	0.0438(9)	0.88(8)
O(9)	0.0173(6)	0.4632(5)	0.1981(9)	0.96(8)
O(10)	0.1447(6)	0.6314(5)	0.3650(9)	0.88(8)
O(11)	− 0.0255(6)	0.7748(5)	0.2707(9)	1.04(8)
O(12)	− 0.1548(6)	0.6050(5)	0.1058(9)	0.96(8)
O(13)	0.4232(6)	0.6050(6)	− 0.011(1)	1.20(8)
O(14)	0.5459(6)	0.6367(5)	0.4559(9)	0.96(8)
O(15)	0.3295(5)	0.6463(5)	0.2668(8)	0.72(8)
O(16)	0.6456(6)	0.5912(5)	0.1635(8)	0.88(8)
O(17)	0.4786(6)	0.4788(5)	0.2753(8)	0.80(8)
O(18)	0.5173(6)	0.7611(5)	0.1917(9)	0.96(8)
O(19)	0.5498(6)	0.8937(5)	− 0.046(1)	1.04(8)
O(20)	0.6986(6)	0.8450(5)	0.3775(9)	1.12(8)
O(21)	0.5387(6)	0.9764(5)	0.2628(9)	0.96(8)
O(22)	0.7375(6)	0.9742(5)	0.1279(9)	0.80(8)
O(23)	0.7271(5)	0.7675(5)	0.0873(8)	0.80(8)
O(24)	0.3049(7)	0.3778(6)	0.116(1)	1.44(8)
O(25)	0.2686(6)	0.2707(5)	0.3784(9)	0.88(8)
O(26)	0.4751(5)	0.2615(5)	0.2708(8)	0.72(8)
O(27)	0.2739(6)	0.4752(5)	0.3916(9)	0.88(8)
O(28)	0.5806(6)	0.1251(6)	0.516(1)	1.20(8)
O(29)	0.3589(5)	0.0893(5)	0.3565(8)	0.80(8)
O(30)	0.6692(5)	0.1488(5)	0.2291(8)	0.72(8)
O(31)	0.6862(6)	0.3640(5)	0.4304(9)	0.88(8)
O(32)	− 0.1680(6)	0.3620(5)	0.200(1)	1.12(8)
O(33)	0.1680(6)	0.8599(6)	0.298(1)	1.20(8)
O(34)	0.6899(6)	0.1249(5)	− 0.0699(9)	1.12(8)
Li(1)	0.142(2)	0.377(2)	0.343(3)	1.8(5)
Li(2)	0.860(2)	0.872(1)	0.155(4)	2.3(6)
Li(3)	0.795(2)	0.254(2)	0.355(3)	2.2(5)
Li(4)	0.692(2)	0.434(2)	0.229(3)	1.9(5)
Li(5)	0.303(2)	− 0.065(2)	0.278(3)	1.8(6)
Li(6)	0.206(2)	0.754(2)	0.145(4)	2.9(6)

Note. Anisotropically refined atoms are given in the form of the isotropic equivalent displacement parameter defined as

$$B = \frac{3}{4}\sum_i\sum_j \mathbf{a}_i\cdot\mathbf{b}_j\cdot\beta_{ij}$$

[a] Atom anisotropically refined.

TABLE 3
X-Ray Powder Diffraction Data of $Li_3Mo_3O_5(PO_4)_3$

h	k	l	d_{obs} (Å)	d_{calc} (Å)	I
1	0	0	11.900	11.860	26.1
1	1	0	8.700	8.696	7.4
1	1	− 1	6.262	6.260	6.8
2	0	0	5.930	5.930	100
1	− 1	1	5.721	5.720	1.7
1	1	1			
2	1	0	5.383	5.385	16.0
0	2	− 1	5.046	5.037	13.5
1	− 2	− 1	4.743	4.740	6.0
2	0	1	4.551	4.556	0.8
2	1	1	4.294	4.292	28.6
0	0	2	4.110	4.107	22.9
1	0	− 2	4.037	4.033	17.7
2	− 2	− 1	3.970	3.968	21.6
0	1	− 2	3.914	3.913	7.2
1	1	− 2	3.859	3.850	11.0
1	− 1	− 2	3.842	3.838	9.8
1	0	2	3.749	3.745	8.4
2	2	1	3.711	3.707	8.4
1	3	− 1	3.657	3.659	2.2
1	− 1	2	3.594	3.594	30.5
0	2	2	3.444	3.444	1.0
3	− 1	1	3.286	3.288	4.6
3	2	− 1	3.239	3.234	19.0
1	2	2	3.225	3.224	25.9
2	0	2	3.203	3.202	25.2
0	4	0	3.182	3.179	88.7
2	3	1	3.106	3.106	7.0
1	4	0	3.074	3.075	2.3
3	2	1	3.000	2.999	13.5
0	4	− 1	2.967	2.969	23.6
1	− 4	0		2.965	
1	3	− 2	2.932	2.930	4.6
1	− 3	− 2	2.916	2.914	4.1
2	4	0	2.811	2.809	11.1
3	− 3	− 1	2.796	2.796	8.7
2	− 4	0			
3	2	− 2	2.747	2.747	1.3
2	− 3	− 2	2.729	2.728	1.8
3	− 3	1	2.654	2.651	11.5
4	2	− 1	2.647	2.646	21.7
3	1	2	2.637	2.634	19.8
4	− 1	1	2.629	2.628	11.7

indexation of the powder pattern of the sample (Table 3) on the basis of the triclinic cell determined from the single crystal study shows its high purity.

Description of the $[Mo_3P_3O_{17}]_\infty$ Framework

The projection of $[Mo_3P_3O_{17}]_\infty$ tridimensional framework along **c** (Fig. 1) shows that it consists of pure octahedral layers $[Mo_8O_{37}]_\infty$ (HTB) and mixed layers $[MoPO_7]_\infty$ built up of corner-sharing octahedra and tetrahedra parallel to (100) and interconnected through PO_4 tetrahedra.

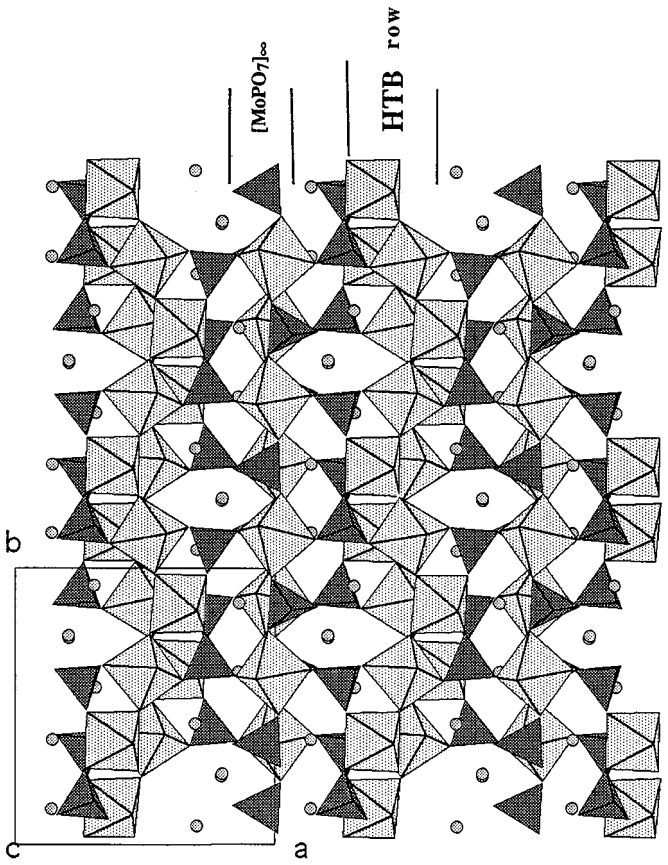

FIG. 1. Projection along **c** of the $Li_3Mo_3O_5(PO_4)_3$ structure.

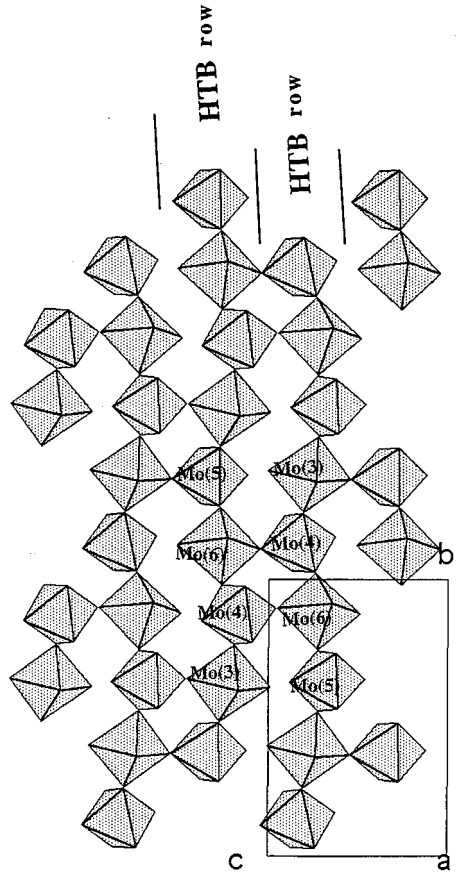

FIG. 2. Projection along **a** of the $[Mo_8O_{37}]_\infty$ layer showing the HTB rows running along **b**.

The $[Mo_8O_{37}]_\infty$ layers are built up of corner-sharing MoO_6 octahedra and form strings that undulate along **b** as shown from the projection of the latter along **a** (Fig. 2). In fact, the geometry of such an octahedral layer is better understood by considering its projection along **c** (Fig. 1). It can be seen that it consists of octahedral rows running along **b** similar to those observed in the hexagonal tungsten bronze (HTB) structure. Two successive HTB rows are stacked along **c** in such a way that they are deduced from each other by a symmetry center; in each HTB row, each octahedron shares only one apex out of two with the two adjacent rows, forming a couple of corner-sharing octahedra "Mo(3) Mo(5)" and "Mo(4) Mo(6)" as shown in Fig. 2.

The $[MoPO_7]_\infty$ layers (Fig. 3) are built up of enanthiomorphic $[MoPO_5]_\infty$ rows running along **b**; in these rows, one PO_4 tetrahedron alternates with one MoO_6 octahedron. In each row two successive tetrahedra, P(2) and P(3), have a trans orientation of their third apex with respect to the row. Two successive enanthiomorphic rows are shifted along **b**, and consequently are linked to each other by the couples of corner-sharing polyhedra "Mo(2) P(2)" and "Mo(1) P(3)," forming S-shaped windows, as represented in Fig. 3.

Two successive $[Mo_8O_{37}]_\infty$ and $[MoPO_7]_\infty$ layers are linked through single PO_4 tetrahedra (P(1), P(4), and P(6)) (Fig. 1). Each of these tetrahedra shares one apex with one octahedron (Mo(1) and Mo(2)) of the $[MoPO_7]_\infty$ layer located above or below, and three apices (for P(4) and P(5)) or two apices (for P(1) and P(6)) with the MoO_6 octahedra of the $[Mo_8O_{37}]_\infty$ layer.

Another simple way to describe the tridimensional $[Mo_3P_3O_{17}]_\infty$ framework is to consider that it results from the stacking along **c** of enanthiomorphic $[Mo_3P_3O_{20}]_\infty$ layers (Fig. 4). These layers that are in fact packed exhibit close relationships with the niobium phosphates bronzes (15) that derive from the HTB structure by replacing MO_6 octahedra by PO_4 tetrahedra. Two successive $[Mo_3P_3O_{20}]_\infty$ layers that are deduced from each other by a symmetry center share the apices of their octahedra (Mo(3), Mo(4), Mo(5), and Mo(6)), and the apices of their octahedra and tetrahedra (Mo(1), Mo(2), P(2), P(3), P(4), and P(5)).

In this tridimensional framework $[Mo_3P_3O_{17}]_\infty$ each PO_4 tetrahedron is linked either to four MoO_6 octahedra,

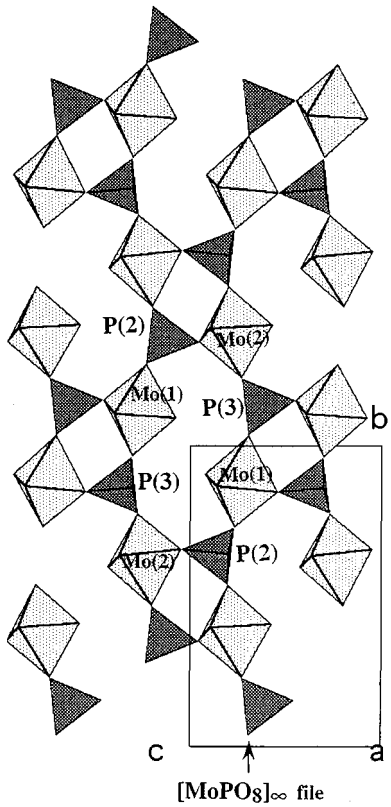

FIG. 3. Projection along **a** of the $[MoPO_7]_\infty$ layer.

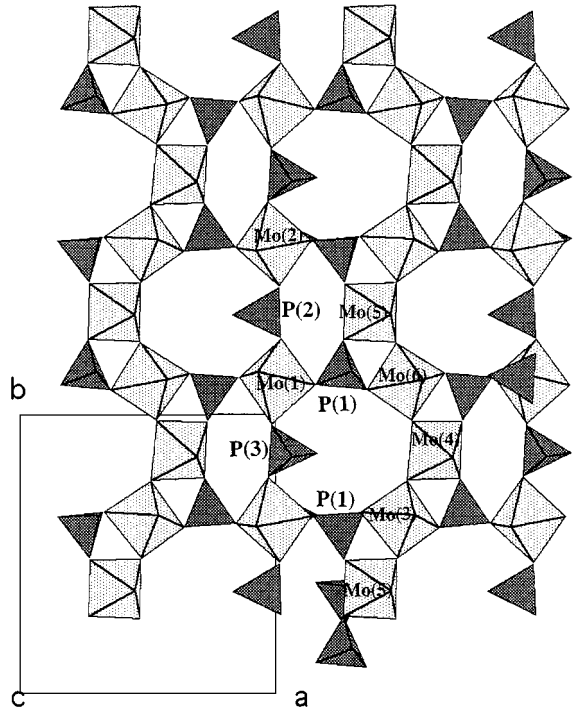

FIG. 4. Projection along **c** of the $[Mo_3P_3O_{20}]_\infty$ layer.

as shown for P(4) and P(5), or to three MoO_6 octahedra, the fourth apex being free as for P(1), P(2), P(3), and P(6). Consequently, this phase can be formulated as a monophosphate $Li_3Mo_3O_5(PO_4)_3$. The interatomic P–O distances are in agreement with those observed in monophosphates (Table 4): the P(4) and P(5) that are linked to four MoO_6 octahedra exhibit P–O distances ranging from 1.485 to 1.570 Å, whereas for the four other types of tetrahedra that exhibit one free apex, the P–O distances are not significantly different, ranging from 1.481 to 1.586 Å.

The consideration of the Mo–O distances in the MoO_6 octahedra is of great interest for the distribution of the electronic charges. The Mo(1) and Mo(2) octahedra that belong to the $[MoPO_7]_\infty$ layers and the Mo(3) and Mo(6) octahedra that belong to the pure octahedral $[Mo_8O_{37}]_\infty$ layers all possess one free apex. For all of them one observes (Table 4) a short Mo–O bond (1.667 to 1.684 Å) opposed to an abnormally long bond (2.155 to 2.339 Å). Such a geometry favors an occupation of these sites by Mo(V) species. This is especially true for the Mo(1) and Mo(2) octahedra, whose equatorial Mo–O distances, ranging from 1.993 to 2.048 Å, are close to those usually observed in Mo(V) octahedra. In contrast, the Mo(3) and Mo(6) octahedra are unusually distorted compared to classical Mo(V) octahedra: one indeed observes two sets of equatorial Mo–O distances ranging from 1.824 to 1.945 Å for the Mo–O–Mo bonds, and from 2.012 to 2.052 Å for the Mo–O–P bonds. The Mo(4) and Mo(5) octahedra that belong to the $[Mo_8O_{37}]_\infty$ layers are linked to three octahedra within the layer and three tetrahedra. They are differently distorted, suggesting a possible occupancy by Mo(VI). The Mo(4) octahedra exhibit three Mo–O shorter distances, ranging from 1.708 to 1.847 Å, that correspond to the Mo–O–Mo bonds, and three longer distances (2.068 to 2.091 Å) corresponding to the Mo–O–P bonds. In the same way, the Mo(5) octahedra are characterized by three Mo–O distances (1.701 to 1.808 Å) corresponding to Mo–O–Mo bonds, the three longer distances (2.059 to 2.087 Å) corresponding to Mo–O–P bonds.

The Lithium Coordination

The $[Mo_3P_3O_{17}]_\infty$ framework forms small elliptic six-sided tunnels running along **c** (Fig. 1) and five-sided tunnels running along **b** (Fig. 5). The lithium cations Li(3) and Li(6) are located at the intersection of these two types of tunnels, where they exhibit a tetrahedral coordination with Li–O distances ranging from 1.94 to 2.19 Å (Table 4). The lithium atoms Li(1) and Li(2) are located in cages between the $[Mo_8O_{37}]_\infty$ and $[MoPO_7]_\infty$ layers, closer to the second type of layers (Fig. 1), where they exhibit a square pyramidal coordination with Li–O distances ranging from 1.95 to 2.18 Å. The lithium cations, Li(4) and Li(5) are also located

TABLE 4
Distances (Å) and Angles (°) in the Polyhedra in $Li_3Mo_3O_5(PO_4)_3$

Mo(1)	O(1)	O(2)	O(3)	O(4)	O(5)	O(6)
O(1)	**1.667(8)**	3.82(1)	2.76(1)	2.74(1)	2.75(1)	3.19(1)
O(2)	176.0(3)	**2.155(7)**	2.70(1)	2.84(1)	2.74(1)	2.819(1)
O(3)	97.2(3)	80.8(3)	**2.003(7)**	3.983(9)	2.727(9)	2.912(9)
O(4)	96.0(3)	85.9(3)	166.7(3)	**2.007(7)**	2.926(9)	2.779(9)
O(5)	95.0(3)	81.4(3)	84.7(2)	92.4(3)	**2.045(6)**	4.037(9)
O(6)	98.9(3)	84.7(3)	92.6(3)	87.1(3)	166.1(3)	**2.026(6)**

Mo(2)	O(7)	O(8)	O(9)	O(10)	O(11)	O(12)
O(7)	**1.680(8)**	3.86(1)	2.84(1)	2.77(1)	2.76(1)	2.75(1)
O(8)	175.8(3)	**2.182(7)**	2.834(9)	2.73(1)	2.75(1)	2.82(1)
O(9)	99.6(3)	84.5(3)	**2.030(7)**	2.878(9)	4.048(9)	2.770(9)
O(10)	97.5(3)	81.4(3)	91.3(3)	**1.995(7)**	2.772(9)	3.958(9)
O(11)	94.9(3)	81.0(3)	165.5(3)	86.6(3)	**2.048(7)**	2.896(9)
O(12)	96.4(3)	84.7(3)	87.0(3)	166.1(3)	91.6(3)	**1.993(7)**

Mo(3)	O(13)	O(14)	O(15)	O(16)	O(17)	O(18)
O(13)	**1.674(8)**	3.98(3)	2.72(1)	2.87(1)	2.87(1)	2.75(1)
O(14)	177.0(3)	**2.308(7)**	2.859(9)	2.88(1)	2.570(9)	2.69(1)
O(15)	94.7(3)	82.6(3)	**2.012(7)**	4.03(1)	2.769(9)	2.81(1)
O(16)	100.3(3)	82.4(3)	164.8(3)	**2.052(7)**	2.71(1)	2.671(9)
O(17)	105.0(3)	73.8(3)	88.8(3)	85.4(3)	**1.945(6)**	3.699(9)
O(18)	101.8(3)	79.7(3)	93.0(3)	86.0(3)	152.9(3)	**1.860(6)**

Mo(4)	O(18)	O(19)	O(20)	O(21)	O(22)	O(23)
O(18)	**1.824(7)**	2.66(1)	2.72(1)	2.804(9)	3.863(9)	3.75(1)
O(19)	97.7(3)	**1.708(8)**	3.79(1)	2.78(1)	2.715(9)	2.777(9)
O(20)	87.7(3)	171.0(3)	**2.091(7)**	2.63(1)	2.73(1)	2.65(1)
O(21)	99.6(3)	102.7(3)	83.5(3)	**1.847(7)**	2.74(1)	3.87(1)
O(22)	165.9(3)	91.4(3)	82.0(3)	88.8(3)	**2.068(7)**	2.649(9)
O(23)	89.3(3)	93.8(3)	78.9(3)	160.0(3)	79.4(3)	**2.080(7)**

Mo(5)	O(17)	O(24)	O(25)	O(26)	O(27)	$O(14)^{i}$
O(17)	**1.808(7)**	2.65(1)	3.82(1)	2.763(9)	2.73(1)	2.72(1)
O(24)	85.5(3)	**2.087(8)**	2.65(1)	2.71(1)	2.65(1)	3.77(1)
O(25)	161.7(3)	79.3(3)	**2.059(7)**	2.72(1)	2.603(9)	2.73(1)
O(26)	100.1(3)	88.2(3)	89.6(3)	**1.795(6)**	3.832(9)	2.64(1)
O(27)	89.2(3)	79.2(3)	78.0(3)	163.7(3)	**2.075(7)**	2.757(9)
$O(14)^{i}$	101.3(3)	169.8(4)	92.5(3)	97.9(3)	93.2(3)	**1.701(7)**

Mo(6)	O(26)	O(28)	O(29)	O(30)	$O(21)^{ii}$	$O(19)^{ii}$
O(26)	**1.934(6)**	2.85(1)	2.737(9)	2.788(9)	3.705(9)	2.70(1)
O(28)	103.9(3)	**1.684(8)**	2.85(1)	2.73(1)	2.82(1)	4.03(1)
O(29)	86.6(3)	99.0(3)	**2.055(7)**	4.05(1)	2.76(1)	2.92(1)
O(30)	89.2(3)	94.7(3)	166.4(3)	**2.021(7)**	2.728(9)	2.913(9)
$O(21)^{iii}$	151.9(3)	104.2(3)	89.1(3)	88.5(3)	**1.885(7)**	2.58(1)
$O(19)^{ii}$	77.7(3)	177.6(3)	82.9(3)	83.5(3)	74.2(3)	**2.339(8)**

P(1)	O(31)	$O(10)^{i}$	$O(15)^{i}$	$O(27)^{i}$
O(31)	**1.497(7)**	2.48(1)	2.54(1)	2.526(9)
$O(10)^{i}$	109.5(4)	**1.534(7)**	2.45(1)	2.508(9)
$O(15)^{i}$	111.9(4)	104.4(4)	**1.567(7)**	2.536(9)
$O(27)^{i}$	112.4(4)	109.1(4)	109.2(4)	**1.544(7)**

TABLE 4—*Continued*

P(2)	O(5)	O(9)	O(32)	$O(8)^{iv}$
O(5)	**1.586(6)**	2.415(9)	2.54(1)	2.568(9)
O(9)	99.2(3)	**1.584(7)**	2.56(1)	2.589(9)
O(32)	111.4(4)	113.0(4)	**1.491(8)**	2.49(1)
$O(8)^{iv}$	110.5(4)	112.0(4)	110.4(4)	**1.539(7)**

P(3)	O(11)	O(33)	$O(6)^{vi}$	$O(2)^{v}$
O(11)	**1.577(6)**	2.54(1)	2.416(9)	2.55(1)
O(33)	111.4(4)	**1.497(8)**	2.55(1)	2.51(1)
$O(6)^{vi}$	100.0(3)	112.0(4)	**1.577(6)**	2.583(9)
$O(2)^{v}$	109.9(4)	111.2(4)	111.8(4)	**1.543(7)**

P(4)	O(4)	O(25)	O(29)	$O(20)^{i}$
O(4)	**1.504(7)**	2.500(9)	2.46(1)	2.46(1)
O(25)	109.7(4)	**1.554(7)**	2.559(9)	2.50(1)
O(29)	106.3(4)	110.0(4)	**1.570(7)**	2.52(1)
$O(20)^{i}$	110.3(4)	109.9(4)	110.6(4)	**1.496(8)**

P(5)	O(24)	$O(12)^{iv}$	$O(16)^{ii}$	$O(23)^{ii}$
O(24)	**1.485(9)**	2.42(1)	2.49(1)	2.49(1)
$O(12)^{iv}$	107.3(4)	**1.518(7)**	2.49(1)	2.495(9)
$O(16)^{ii}$	109.1(4)	107.9(4)	**1.568(7)**	2.558(9)
$O(23)^{ii}$	111.4(4)	109.8(4)	111.2(4)	**1.532(7)**

P(6)	O(30)	O(34)	$O(22)^{iii}$	$O(3)^{vii}$
O(30)	**1.563(7)**	2.51(1)	2.538(9)	2.46(1)
O(34)	110.9(4)	**1.481(8)**	2.53(1)	2.46(1)
$O(22)^{iii}$	109.6(4)	113.6(4)	**1.542(7)**	2.486(9)
$O(3)^{vii}$	105.1(4)	109.2(4)	107.9(4)	**1.533(7)**

Li(1)–O(5) : 2.05(2)
Li(1)–O(7)^{v} : 2.16(3)
Li(1)–O(9) : 2.10(2)
Li(1)–O(25) : 2.03(2)
Li(1)–O(27) : 2.02(2)

Li(2)–O(1)^{ii} : 2.18(3)
Li(2)–O(6)^{viii} : 2.16(2)
Li(2)–O(11)^{vii} : 2.00(2)
Li(2)–O(22) : 1.95(2)
Li(2)–O(23) : 2.09(2)

Li(3)–O(2)^{vii} : 2.19(2)
Li(3)–O(30) : 2.18(2)
Li(3)–O(31) : 2.05(2)
Li(3)–O(32)^{vii} : 1.97(3)

Li(4)–O(13)^{ii} : 2.19(2)
Li(4)–O(16) : 2.13(2)
Li(4)–O(31) : 1.90(2)
Li(4)–O(32)^{vii} : 1.95(3)

Li(5)–O(28)^{ix} : 2.20(2)
Li(5)–O(29) : 2.15(2)
Li(5)–O(33)^{iii} : 1.90(2)
Li(5)–O(34)^{x} : 1.92(3)

Li(6)–O(8) : 2.19(3)
Li(6)–O(15) : 2.17(3)
Li(6)–O(33) : 1.94(3)
Li(6)–O(34)^{ii} : 2.14(3)

O(5)–Li(1)–O(7)^{v} : 101.5(9)
O(5)–Li(1)–O(9) : 71.0(6)
O(5)–Li(1)–O(25) : 95.5(9)
O(5)–Li(1)–O(27) : 163.5(8)
O(7)^{v}–Li(1)–O(9) : 71.0(6)
O(7)^{v}–Li(1)–O(25) : 71.0(6)
O(7)^{v}–Li(1)–O(27) : 71.0(6)
O(9)^{v}–Li(1)–O(25) : 153.4(7)
O(9)^{v}–Li(1)–O(27) : 106.0(9)
O(25)–Li(1)–O(27) : 80.2(8)

O(1)^{ii}–Li(2)–O(6)^{viii} : 94.6(8)
O(1)^{ii}–Li(2)–O(11)^{vii} : 104.4(9)
O(1)^{ii}–Li(2)–O(22) : 96.1(6)
O(1)^{ii}–Li(2)–O(23) : 104.0(9)
O(6)^{viii}–Li(2)–O(11)^{vii} : 71.0(8)
O(6)^{viii}–Li(2)–O(22) : 99.3(7)
O(6)^{viii}–Li(2)–O(23) : 161(1)
O(11)^{vii}–Li(2)–O(22) : 158(1)
O(11)^{vii}–Li(2)–O(23) : 101.1(8)
O(22)–Li(2)–O(23) : 81.8(8)

O(2)^{vii}–Li(3)–O(30) : 105.9(9)
O(2)^{vii}–Li(3)–O(31) : 139.5(6)
O(2)^{vii}–Li(3)–O(32)^{vii} : 116(1)
O(30)–Li(3)–O(31) : 98.1(9)
O(30)–Li(3)–O(32)^{vii} : 108.6(5)
O(31)–Li(3)–O(32)^{vii} : 85.8(9)

O(13)^{ii}–Li(4)–O(16) : 83.8(6)
O(13)^{ii}–Li(4)–O(31) : 122(1)
O(13)^{ii}–Li(4)–O(32)^{vii} : 104.9(7)
O(16)–Li(4)–O(31) : 128.7(9)
O(16)–Li(4)–O(32)^{vii} : 128(1)
O(31)–Li(4)–O(32)^{vii} : 90.6(8)

TABLE 4—*Continued*

$O(28)^{ix}$–Li(5)–O(29) : 86.3(6)	O(8)–Li(6)–O(15) : 105(1)
$O(28)^{ix}$–Li(5)–$O(33)^{iii}$: 103.1(7)	O(8)–Li(6)–O(33) : 116(1)
$O(28)^{ix}$–Li(5)–$O(34)^{x}$: 119(1)	O(8)–Li(6)–$O(34)^{ii}$: 138.9(7)
O(29)–Li(5)–$O(33)^{iii}$: 132(1)	O(15)–Li(6)–O(33) : 109.5(5)
O(29)–Li(5)–$O(34)^{x}$: 126.3(9)	O(15)–Li(6)–$O(34)^{ii}$: 102(1)
$O(33)^{iii}$–Li(5)–$O(34)^{x}$: 90.4(8)	O(33)–Li(6)–$O(34)^{ii}$: 84(1)

Note. The Mo–O or P–O distances are on the diagonal, above them are the O ⋯ O distances and below them are the O–Mo–O or O–P–O angles.

Symmetry codes. (i) $x+1, y+1, z+1$; (ii) $x+1, y+1, z$; (iii) $-x, -y-1, -z$; (iv) $x, y+1, z$; (v) $x, y+1, z$; (vi) $-x, -y+1, -z$; (vii) $-x-1, -y, -z$; (viii) $-x-1, -y+1, -z$; (ix) $x+1, y, z+1$; (x) $x+1, y, z$.

in cages between the $[Mo_8O_{37}]_\infty$ and $[MoPO_7]_\infty$ layers but closer to the first type of layer (Fig. 1); like Li(1) and Li(2) they exhibit a tetrahedral coordination with Li–O distances ranging from 1.90 to 2.20 Å.

Distribution of Electrons over the Mo Octahedra and Magnetic Properties

The existence of layers of corner-sharing MoO_6 octahedra raises the issue of the distribution of electrons within these layers, i.e., of the competition between electronic delocalization and charge ordering.

As pointed out in the structural study, it appears that the Mo(V) and Mo(VI) species, even in the pure octahedral $[Mo_8O_{37}]_\infty$ layers, are arranged in an ordered way. This viewpoint is also supported by the bond valence calculations using the Altermatt and Brown theory (16). One indeed obtains (Table 5) calculated valencies of $+4.97$ and $+4.91$ for the molybdenum atoms Mo(1) and Mo(2) of the $[MoPO_7]_\infty$ layers, indicating that in these layers molybdenum is essentially pentavalent. In the $[Mo_8O_{37}]_\infty$ layers, the Mo(3) and Mo(6) atoms exhibit calculated valencies of $+5.26$ and $+5.13$, respectively, whereas the

TABLE 5
Electrostatic Valences for $Li_3Mo_3O_5(PO_4)_3$

	Mo(1)	Mo(2)	Mo(3)	Mo(4)	Mo(5)	Mo(6)	P(1)	P(2)	P(3)	P(4)	P(5)	P(6)	Li(1)	Li(2)	Li(3)	Li(4)	Li(5)	Li(6)	$\sum vi^-$
O(1)	1.773													0.145					1.918
O(2)	0.474								1.179						0.143				1.937
O(3)	0.715											1.212							1.927
O(4)	0.707									1.310									2.017
O(5)	0.638												0.206						1.894
O(6)	0.672								1.076					0.153					1.901
O(7)		1.712						1.050					0.153						1.865
O(8)		0.441						1.192										0.141	1.774
O(9)		0.665						1.055					0.180						1.900
O(10)		0.731					1.208												1.939
O(11)		0.633							1.076					0.236					1.945
O(12)		0.735									1.262								1.997
O(13)			1.740													0.141			1.881
O(14)			0.313		1.745														2.058
O(15)			0.698				1.105											0.149	1.952
O(16)			0.626								1.102					0.166			1.894
O(17)			0.836		1.307														2.143
O(18)			1.052	1.251															2.303
O(19)				1.712		0.288													2.000
O(20)				0.608						1.339									1.947
O(21)				1.176		0.984													2.160
O(22)				0.647								1.182							1.829
O(23)				0.626							1.215			0.270					2.111
O(24)					0.615						1.379			0.185					2.179
O(25)					0.663					1.145			0.218						2.026
O(26)					1.353	0.862													2.215
O(27)					0.635		1.176						0.224						2.035
O(28)						1.694											0.138		1.832
O(29)						0.621				1.096							0.157		1.874
O(30)						0.681						1.117			0.145				1.943
O(31)							1.335								0.206	0.309			1.850
O(32)								1.357							0.256	0.270			1.883
O(33)									1.335								0.309	0.278	1.922
O(34)												1.394					0.293	0.162	1.849
$\sum vi^+$	4.979	4.917	5.265	6.02	6.318	5.130	4.824	4.654	4.666	4.890	4.958	4.905	0.981	0.989	0.891	0.886	0.897	0.730	

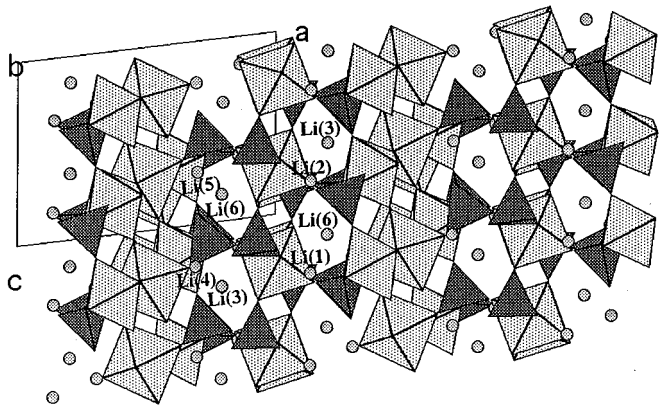

FIG. 5. Projection along **b** of the $Li_3Mo_3O_5(PO_4)_3$ structure.

Mo(4) and Mo(5) atoms exhibit valencies of $+6.02$ and $+6.31$, respectively. Such results indicate a large tendency to an ordering of the Mo(V) and Mo(VI) species within those layers.

The evolution of the molar reciprocal susceptibility versus temperature shows that above 10 K the curve $\chi^{-1}(T)$ can be fitted with the law $\chi = \chi_0 + C_m/(T - \theta)$ (Fig. 6a). However, the fitting parameter of 1.53 μ_B for 2 Mo(V) per molar unit $Li_3Mo^{VI}Mo_2^{V}O_5(PO_4)_3$ is significantly lower than the theoretical parameter (1.73 μ_B). Consequently, some electronic delocalization within the $[Mo_8O_{37}]_\infty$ layers exists in spite of the bond valence calculations. This partial electronic delocalization is also supported by the electrical resistivity of 3.6×10^4 Ω cm at room temperature, measured on a sintered bar of this material. Thus a semiconducting behavior along the (100) plane can be expected. At low temperature, i.e., for $T < 7$ K for curve $\chi^{-1}(T)$ (Fig. 6b) shows an antiferromagnetic ordering which is in agreement with the existence of the several different possible sites for Mo(V) in both the $[Mo_8O_{37}]_\infty$ and $[MoPO_7]_\infty$ layers.

CONCLUSION

A new mixed-valent molybdenum monophosphate with a high Mo(V)/Mo(VI) molar ratio has been isolated. This

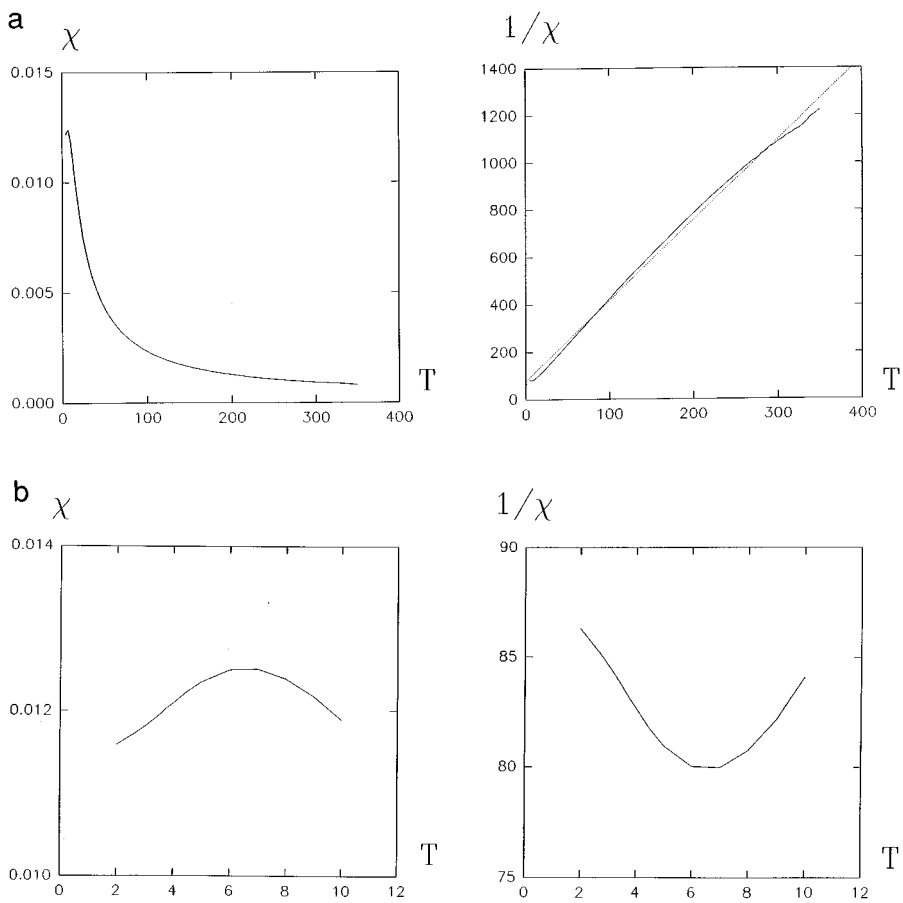

FIG. 6. (a) The magnetic susceptibility χ and $1/\chi$ versus T(K) for $4.5 < T < 300$ K. (b) The magnetic susceptibility χ and $1/\chi$ versus T(K) for $4.5 < T < 10$ K.

phase is unique in that it exhibits infinite layers of corner-sharing MoO_6 octahedra. This structural behavior is in contrast to other mixed-valent molybdenum phosphates that are all characterized by isolated octahedral units which are interconnected through phosphate groups. A strong tendency to ordering is predicted for the Mo(V) and Mo(VI) species according to the interatomic distances and bond valence calculations. Nevertheless, the magnetic study suggests a partial delocalization above 10 K, whereas an antiferromagnetic order is observed below this temperature. These observations suggest a possible anisotropy of the transport properties of this material which is in agreement with the existence of octahedral Mo layers. The growth of larger single crystals will be necessary in order to understand the electronic distribution in this compound.

REFERENCES

1. S. Ledain, A. Leclaire, M. M. Borel, and B. Raveau, *J. Solid State Chem.* **122,** 107 (1996).
2. S. Ledain, A. Leclaire, M. M. Borel, and B. Raveau, *J. Solid State Chem.* **124,** 322 (1996).
3. M. M. Borel, A. Leclaire, A Grandin, and B. Raveau, *J. Solid State Chem* **108,** 336 (1994).
4. M. M. Borel, A. Leclaire, A. Guesdon, A. Grandin, and B. Raveau, *J. Solid State Chem* **112,** 15 (1994).
5. T. Hoareau, A. Leclaire, M. M. Borel, A. Grandin, and B. Raveau, *Eur. J. Solid State Inorg. Chem.* **112,** 15 (1994).
6. T. Hoareau, A. Leclaire, M. M. Borel, A. Grandin, and B. Raveau, *J. Solid State Inorg. Chem.* **116,** 87 (1994).
7. G. Costentin, M. M. Borel, A. Leclaire, A. Grandin, and B. Raveau, *J. Solid State Chem.* **95,** 168 (1991).
8. A. Guesdon, M. M. Borel, A. Leclaire, A. Grandin, and B. Raveau, *C. R. Acad. Sci.* **316,** 477 (1993).
9. T. Hoareau, A. Leclaire, M. M. Borel, J. Provost, and B. Raveau, *Mat. Res. Bull.* **30,** 523 (1995).
10. A Guesdon, M. M. Borel, A. Leclaire, A. Grandin, and B. Raveau, *J. Solid State Chem.* **109,** 145 (1994).
11. M. M. Borel, A. Guesdon, A. Leclaire, A. Grandin, and B. Raveau, *Zeit. Anorg. All. Chem.* **620,** 569 (1994).
12. T. Hoareau, A. Leclaire, M. M. Borel, J. Provost, and B. Raveau, *J. Solid State Chem.* **128,** 233 (1997).
13. S. Ledain, M. M. Borel, A. Leclaire, J. Provost, and B. Raveau, *J. Solid State Chem.* **120,** 260 (1995).
14. S. Ledain, M. M. Borel, A. Leclaire, and B. Raveau, *Mat. Chem.* [submitted]
15. B. Raveau, M. M. Borel, A. Leclaire, and A. Grandin, *Int. J. Modern Phys. B* **7,** 4109 (1993).
16. I. D. Brown and D. Altermatt, *Acta Crystallogr. B* **41,** 244 (1985).